Pressure-Induced Transition from Localized Electron Toward Band Antiferromagnetism in $LaMnO_3$

J.-S. Zhou and J. B. Goodenough

Texas Materials Institute, ETC 9.102, University of Texas at Austin, Austin, Texas 78712

(Received 9 January 2002; published 2 August 2002)

The temperature dependence of the ac susceptibility under pressure has been used to track the Néel temperature T_N of the Mott insulators $LaMnO_3$, $CaMnO_3$, and $YCrO_3$. Bloch's rule relating T_N to volume V, viz., $\alpha = d\log T_N/d\log V = -3.3$, is obeyed in $YCrO_3$ and $CaMnO_3$; it fails in $LaMnO_3$. This breakdown is interpreted to be due to a sharp increase in the factor $[U^{-1} + (2\Delta)^{-1}]$ entering the superexchange perturbation formula. A first-order change at 7 kbar indicates that the transition from localized-electron to band magnetism is not smooth.

DOI: 10.1103/PhysRevLett.89.087201 PACS numbers: 75.30.Et, 71.27.+a, 71.28.+d, 71.70.Gm

A cooperative Jahn-Teller distortion of the high-spin $Mn(III)O_{6/2}$ octahedra below $T_{JT} = 700$ K makes $LaMnO_3$ an insulator with type-A antiferromagnetic order below $T_N = 140$ K. On the other hand, our previous demonstration [1] of an insulator-conductive transition at T_{JT} in $LaMnO_3$ has indicated that the on-site correlation energy U_σ for the σ bonding e electron in this compound is not sufficiently large to prevent charge disproportionation at $T > T_{JT}$. Ahn and Millis [2] have subsequently argued that the superexchange perturbation formula may not be applicable in this small-U compound. In this Letter, we demonstrate that the spin-spin interactions approach the transition from localized-electron to band magnetism where the superexchange perturbation description breaks down under high pressure.

Bloch [3] studied the variation of T_N and volume V of numerous antiferromagnetic insulators and found the general relationship $\alpha = d\log T_N/d\log V = -3.3$. In the localized-electron limit where the superexchange perturbation approach is applicable, theory gives $T_N \sim b^2[U^{-1} + (2\Delta)^{-1}]$, where the metal-metal electron-transfer energy integral in an AMO_3 perovskite, $b \approx (b^{ca})^2/\Delta$, contains the anion-cation back-transfer integral b^{ca} and the O-2p to lowest M-3d charge-transfer gap Δ. The first term in the expression for T_N is the Anderson superexchange term; the second involves a two-electron transfer from an O^{2-} ion, one to each of the two interacting cations on opposite sides of it. A theoretical rationalization of the Bloch rule comes from calculations [4,5] of the variation of the overlap integral in b^{ca} with the cation-anion bond length r; it varies as r^{-n} with a calculated $n = 2.5$–3, which makes $T_N \sim r^{-10}$–$V^{-3.3}$ and therefore $\alpha = -3.3$ if U and Δ remain independent of r or V. The perturbation description for the superexchange spin-spin interaction should break down on the approach to crossover from localized to itinerant electronic behavior of a Mott-Hubbard insulator. However, experimental examples of crossover are rare. Aronson *et al.* [6] obtained an $\alpha = d\log J/d\log r < 10$ from a measurement of the pressure dependence of the exchange parameter J on one sample $La_2CuO_{4+\delta}$ ($T_N = 308$ K) and high-pressure structural data on another sample of $La_2CuO_{4+\delta}$ [7]. The smaller α than expected from the Bloch rule led Aronson *et al.* to conclude that a nonperturbative calculation of the magnetic-exchange energy is needed for this compound. Although a subsequent measurement [8] on an La_2CuO_4 sample with $T_N = 320$ K has shown a higher $d\log T_N/dP$, it appears that antiferromagnetic La_2CuO_4 is at the crossover from localized to itinerant electronic behavior.

Single-crystal samples of $LaMnO_3$ and $CaMnO_3$ were grown in an infrared-heating image furnace from ceramic bars. A gas flow at 1 atm of argon and 2 atm oxygen pressure were used in the crystal growth of $LaMnO_3$ and $CaMnO_3$, respectively. The ceramic sample $YCrO_3$ was synthesized by solid-state reaction. All samples were single-phase to x-ray powder diffraction and are oxygen stoichiometric to within 0.1% by measurement of thermoelectric power. The dc magnetization of these samples was obtained with a SQUID magnetometer; the ac susceptibility under pressure was measured in a self-clamped Be-Cu cylinder with internal primary/secondary coils and silicone oil as the pressure medium. The primary coil was powered by a 5 kHz ac current that generated a magnetic field of about 4 Oe at the sample. All measurements made under pressure used the same coils. The pressure inside the pressure cell was monitored with a manganin pressure manometer. The labeled pressures in the figures are those measured at T_N.

Figure 1 for $YCrO_3$ shows the dc magnetization in a field $H = 35$ Oe and the ac susceptibility at ambient pressure. The sharp peak in the ac susceptibility $\chi(T)$ at T_N should not be taken as evidence of spin-glass behavior since the typical features in the temperature dependence of the zero-field-cooled and field-cooled dc magnetization are lacking. We use the peak in $\chi(T)$ to monitor the pressure dependence of T_N. Pressure does not change the antiferromagnetic ordering in $YCrO_3$ (G type), $CaMnO_3$ (G type), and $LaMnO_3$ (A type), but it increases the transition temperature T_N as shown in Fig. 2. A broadening of the $\chi(T)$ peak is greater in the polycrystalline $YCrO_3$ sample than in the

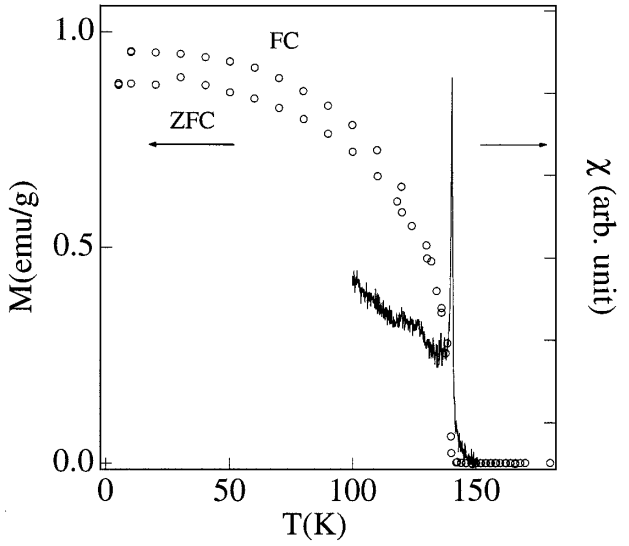

FIG. 1. Temperature dependence of the dc magnetization at $H = 35$ Oe together with $\chi_{ac}(T)$ under ambient pressure for $YCrO_3$.

single-crystal samples $CaMnO_3$ and $LaMnO_3$. The slight broadening of the peaks in the single-crystal samples may be caused by a nonhydrostatic pressure, but the abrupt change in the peak profile near 7 kbar in $LaMnO_3$ is intrinsic. As can be seen in Fig. 3, which shows the pressure dependences of T_N for the three samples, T_N varies linearly with P over the entire pressure range for $YCrO_3$ and $CaMnO_3$, but only in the range $P > 7$ kbar for $LaMnO_3$. Moreover, a close examination of the $\chi(T)$ peaks for $LaMnO_3$ near 7 kbar shows the existence of two peaks, indicating a two-phase region characteristic of a first-order phase change at 7 kbar. A $dT_N/dP = 0.34$ K/kbar for $CaMnO_3$ and 0.30 K/kbar for $YCrO_3$ obtained from Fig. 3 are a little smaller than the respective 0.41 K/kbar and 0.38 K/kbar values previously reported [9]. This difference may be attributed to such factors as a smaller pressure range $P < 8$ kbar, fewer data points, and a somewhat lower quality polycrystalline $CaMnO_3$ sample in the earlier work. To our knowledge, the pressure dependence of T_N in $LaMnO_3$ has not been previously measured. In contrast to $CaMnO_3$ and $YCrO_3$, the curve of T_N versus P for $LaMnO_3$ is not only nonlinear below 7 kbar with an abrupt change in dT_N/dP at the first-order phase change at 7 kbar; it also shows a high slope $dT_N/dP = 0.55$ K/kbar at pressures $P > 7$ kbar.

The Mn(IV) and Cr(III) ions of $CaMnO_3$ and $YCrO_3$ each have t^3e^0 cubic-field d-electron configurations, which leads to isotropic t^3-O-t^3 antiferromagnetic interactions and G-type antiferromagnetic order. The effective U_π for these compounds contains an intra-atomic exchange energy Δ_{ex}, which makes it larger than 3 eV. Qualitatively, the $dT_N/dP > 0$ found for $YCrO_3$ and $CaMnO_3$ fits the behavior of localized t^3 configurations with superexchange spin-spin interactions [9].

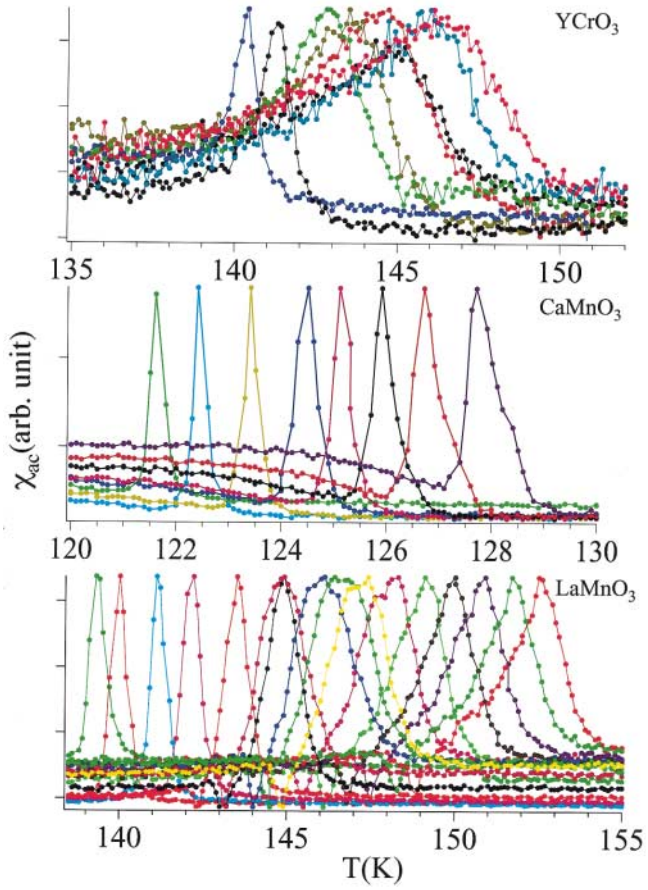

FIG. 2 (color). Temperature dependence of the ac susceptibility χ for $LaMnO_3$, $CaMnO_3$, and $YCrO_3$ under different pressures. The pressure values measured at the temperature of maximum $\chi(T)$, which corresponds to T_N, can be read from Fig. 3.

The unusual pressure dependence of T_N found in $LaMnO_3$ might originate in the behavior of the e electron of the Mn(III) : t^3e^1 manifold. A cooperative Jahn-Teller distortion orders the e electrons into the (001) planes where they give rise to ferromagnetic interactions, and the A-type antiferromagnetic order is due to the t^3-O-t^3 interactions between ferromagnetic (001) planes [10]. The cooperative ordering of the occupied e orbitals into the (001) planes has been shown by neutron-diffraction made under pressure [11] to remain stable to 70 kbar; the A-type magnetic order is retained over the pressure range of this study. Application of hydrostatic pressure on the orthorhombic $Pbnm$ perovskite could change the $(180° - \phi)$ Mn-O-Mn bond angles. Boekema *et al.* [12] have shown a linear dependence between T_N and $\cos^2\theta$ as predicted from superexchange theory, where the angle $\theta = (180° - \phi)$ is changed by chemical pressure, i.e., by altering the tolerance factor through changing the mean radius of the A cation of AMO_3 perovskites. In $Sr_{1-x}Ca_xMnO_3$, a $dT_N/d\langle\cos^2\theta\rangle = 587$ K [13], in $RFeO_3$ (R = rare earth element) a $dT_N/d\langle\cos^2\theta\rangle = 479$ K [14], and in $RMnO_3$ a

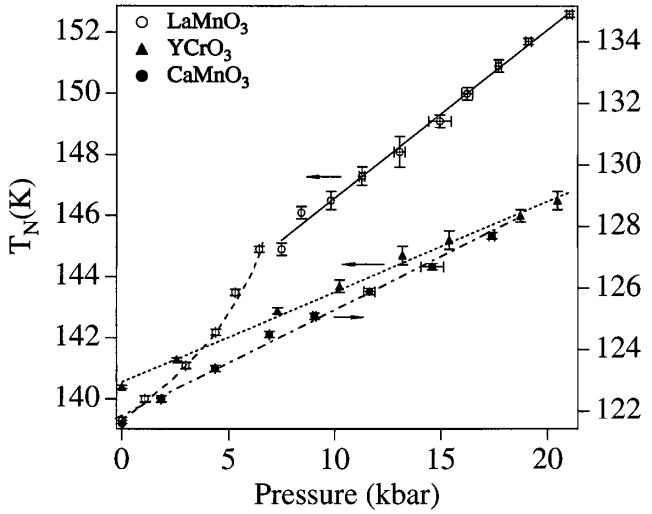

FIG. 3. Pressure dependence of the Néel temperature for $LaMnO_3$, $CaMnO_3$, and $YCrO_3$. Linear fittings have been made for $CaMnO_3$, $YCrO_3$, and $LaMnO_3$ at $P > 7$ kbar.

$dT_N/d\langle\cos^2\theta\rangle = 890$ K [13] have been found. In order to test whether the pressure dependence of T_N in $LaMnO_3$ can be described by superexchange perturbation theory, it is necessary to turn to Bloch's rule.

The double log plot of T_N versus V of Fig. 4 was obtained with the aid of neutron-diffraction data [11] taken on an $LaMnO_3$ sample of similar quality to that on which

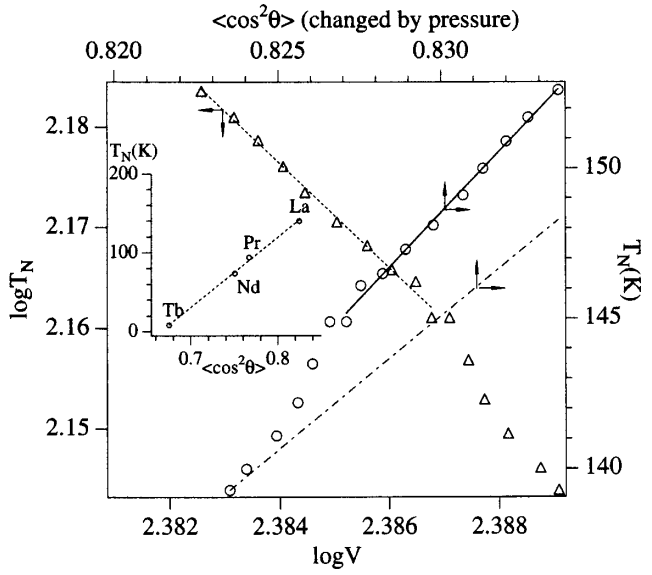

FIG. 4. Double log plot of the Néel temperature versus the volume and the $\langle\cos^2\theta\rangle$ dependence of T_N for $LaMnO_3$. The dashed line is a linear fit of the curve of $\log T_N$ versus $\log V$, which gives an $\alpha_B = -5.3$. The dot-dashed line with a slope $dT_N/d\langle\cos^2\theta\rangle = 890$ is taken from the curve of T_N vs $\langle\cos^2\theta\rangle$ obtained by chemical substitution shown as an inset after Ref. [13]. The solid line with a slope $dT_N/d\langle\cos^2\theta\rangle = 1148$ is a linear fit to the curve of T_N versus $\langle\cos^2\theta\rangle$ changed by pressure.

we measured T_N versus P. A linear fit applies in the pressure range $P > 7$ kbar; it gives an $\alpha = -5.1$, which is much higher in magnitude than the $\alpha = -3.3$ expected from Bloch's rule. A large $|\alpha|$ indicates either T_N or the volume V has an unusual pressure dependence. High-pressure neutron-diffraction shows a compressibility $\kappa = -0.70 \times 10^{-6}$/bar for $LaMnO_3$, which is in line with $K = -0.68 \times 10^{-6}$/bar obtained by Bloch on many antiferromagnetic insulators [3]. Therefore we may conclude that the anomalously large magnitude of α in $LaMnO_3$ is due to an unusually large pressure dependence of T_N. The data for $LaMnO_3$ together with those for $CaMnO_3$ and $YCrO_3$ are listed in Table I for comparison.

The pressure dependence of the overlap integral b^{ca}, i.e., $db^{ca}/dP \sim \kappa/V$, can be obtained from the calculation $b^{ca} \sim r^{-n}$ ($n = 2.5$–3) [4,5]. Since κ for $LaMnO_3$ is not anomalous, we conclude that the deviation from Bloch's rule in $LaMnO_3$ with an $|\alpha| > 3.3$ is due to the factor $[U^{-1} + (2\Delta)^{-1}]$ in the superexchange perturbation expression; this factor increases with the bandwidth in $LaMnO_3$. On the approach to crossover from localized-electron to band magnetism, we can expect U to decrease sharply with increasing W as a result of a feedback-augmented screening of U until a first-order collapse occurs at a critical bandwidth where the equilibrium M-O bond length has a double-well potential. The phase with nonlinear dT_N/dP below 7 kbar can be assigned to a region where the factor $[U^{-1} + (2\Delta)^{-1}]$ increases with pressure. A narrow two-phase region is observed in the interval $7 \leq P \leq 10$ kbar, and the high-pressure phase has a constant dT_N/dP. Preliminary data at a pressure a little over the limit of the Be-Cu chamber suggests another two-phase region associated with a second first-order transition. The high-T_N phase does not yet contain long-range-itinerant electrons in the (001) planes, but it may contain molecular orbitals within Mn-O-Mn bonds.

The fact that the magnetic-exchange interactions in $LaMnO_3$ are anisotropic, whereas those of $CaMnO_3$ and $YCrO_3$ are isotropic, might be considered the origin of the unusually large $|\alpha|$. We note that the ferromagnetic in-plane interactions do not compete with the antiferromagnetic interactions between planes, and that decreasing the Mn-O-Mn bond angle θ with substitutions of smaller lanthanides for La gives the $T_N \sim \langle\cos^2\rangle\theta$ dependence, Fig. 4, anticipated by the perturbation theory. Application of hydrostatic pressure on $LaMnO_3$ increases the angles θ monotonically [11]. Therefore, pressure plays the same role as chemical substitution. However, as shown in Fig. 4, the relation between T_N and $\langle\cos^2\theta\rangle$ deviates dramatically from that of $T_N \sim \langle\cos^2\theta\rangle$ as $\langle\cos^2\theta\rangle$ is increased under pressure in $LaMnO_3$. T_N vs $\langle\cos^2\theta\rangle$ has a much greater slope under a pressure $P > 7$ kbar.

In contrast to $LaMnO_3$, $YCrO_3$ obeys the Bloch rule as expected for a localized-electron antiferromagnet with a $[U^{-1} + (2\Delta)^{-1}]$ that varies little with pressure in the pressure range studied. $CaMnO_3$ appears to approach the

TABLE I. The Bloch parameter, compressibility, and pressure dependence of T_N.

	$\lvert\alpha\rvert = d(\log T_N)/d(\log V)$[a]	$\lvert K\rvert = (1/V)dV/dP$ (bar^{-1})	$(1/T_N)dT_N/dP$ (bar^{-1})
$LaMnO_3$	5.3	0.70×10^{-6}[c]	3.9×10^{-6}
$CaMnO_3$	3.8[b]	0.68×10^{-6}[d]	2.7×10^{-6}
$YCrO_3$	3.0[b]	0.68×10^{-6}[d]	2.1×10^{-6}

[a] $|\alpha| \approx 3.3$ in Bloch's rule.
[b] α is calculated by using $K = 0.68 \times 10^{-6}$.
[c] Measured result of $LaMnO_3$.
[d] The compressibility found in magnetic insulators.

threshold for breakdown of the assumption $[U^{-1} + (2\Delta)^{-1}] \approx$ const because the small Δ in this compound may vary with pressure. A $dT_N/dP < 0$ found for the insulator $CaCrO_3$ was interpreted to locate this perovskite in the regime of band antiferromagnetism since $SrCrO_3$ is a Pauli paramagnetic metal [15]. We therefore tentatively place these compounds in the schematic plot of exchange energy J versus bandwidth W shown in Fig. 5. As the two-phase region is approached in $LaMnO_3$, a feedback-enhanced decrease of U_σ with increasing W causes the Bloch rule and the perturbation method to break down. The transition from localized to itinerant electronic behavior appears to proceed in $LaMnO_3$ by at least one intermediate step.

In conclusion, the smaller U in $LaMnO_3$ than U_π in $CaMnO_3$ and $YCrO_3$ makes $LaMnO_3$ a promising candidate for exploration of the breakdown of the superexchange perturbation theory. The Bloch rule for localized-electron antiferromagnetism, viz., $\alpha = d\log T_N/d\log V \approx -3.3$, provides a test of the application of the superexchange perturbation method and of how it breaks down. $YCrO_3$ was found to obey the Bloch rule; $CaMnO_3$ did also, but it appears to approach the limit where the factor $[U^{-1} + (2\Delta)^{-1}]$ of the perturbation theory can be assumed to be independent of pressure. By comparison, $LaMnO_3$ has an unusually large value of dT_N/dP that has little to do with either the compressibility or the cooperative Jahn-Teller distortion. A nonlinear behavior of α in the range $P < 7$ kbar and a first-order phase change at $P \approx 7$ kbar is followed for $P > 7$ kbar by an $|\alpha| = 5.3$, which is significantly larger than the Bloch-rule value. This behavior is consistent with a breakdown of the superexchange perturbation method as a result of a dramatic decrease in U with pressure, a decrease resulting from a feedback enhancement of the screening of the on-site electron-electron Coulomb energy U as the transition from localized-electron to band ferromagnetism is approached.

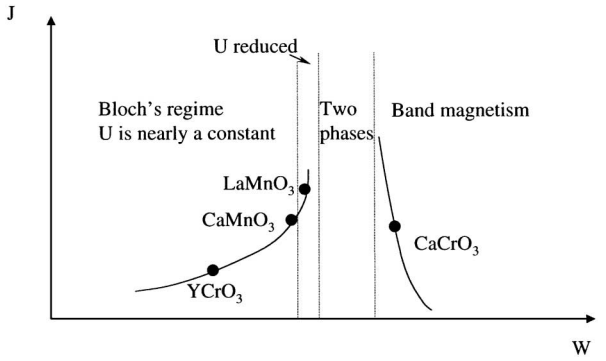

FIG. 5. A schematic diagram of the Heisenberg magnetic-exchange energy J versus bandwidth W at the crossover from localized-electron to the band magnetism.

We acknowledge the financial support of the NSF (DMR0132282), the TCSUH of Houston, Texas, and the Robert A. Welch Foundation of Houston, Texas.

[1] J.-S. Zhou and J. B. Goodenough, Phys. Rev. B **60**, R15002 (1998).
[2] K. H. Ahn and A. J. Millis, Phys. Rev. B **64**, 115103 (2001).
[3] D. Bloch, J. Phys. Chem. Solids **27**, 881 (1966).
[4] K. N. Shrivastava and V. Jaccarino, Phys. Rev. B **13**, 299 (1976).
[5] D. W. Smith, J. Chem. Phys. **50**, 2784 (1969).
[6] M. C. Aronson, S. B. Dierker, B. S. Dennis, S.-W. Cheong, and Z. Fisk, Phys. Rev. B **44**, 4657 (1991).
[7] M. J. Akhtart, C. R. A. Catlow, S. M. Clark, and W. M. Temmerman, J. Phys. C **21**, L917 (1988).
[8] V. Doroshev, V. Krivoruchko, M. Savosta, A. Shestakov, and T. Tarasenko, J. Magn. Magn. Mater. **157/158**, 669 (1996).
[9] N. Menyuk, J. A. Kafalas, K. Dwight, and J. B. Goodenough, J. Appl. Phys. **40**, 1324 (1969).
[10] J. B. Goodenough, Phys. Rev. **100**, 564 (1955).
[11] L. Pinsard-Gaudart, J. Rodriguez-Carvajal, A. Daoud-Aladine, I. Goncharenko, M. Medarde, R I. Smith, and A. Revcolevschi, Phys. Rev. B **64**, 064426 (2001).
[12] C. Boekema, F. Van Der Woude, and G. A. Sawatzky, Int. J. Magn. **3**, 341 (1972).
[13] O. Chmaissem, B. Dabrowski, S. Kolesnik, J. Mais, D. E. Brown, R. Kruk, P. Prior, B. Pyles, and J. D. Jorgensen, Phys. Rev. B **64**, 134412 (2001).
[14] D. Treves, M. Eibschutz, and P. Coppens, Phys. Lett. **18**, 216 (1966).
[15] J. B. Goodenough, J. M. Longo, and J. A. Kafalas, Mater. Res. Bull. **3**, 471 (1968).